

Raman spectra and DFT calculations for tetraterpene hydrocarbons from the L race of the green microalga *Botryococcus braunii*



Hye Jin Chun ^{a,1}, Sergio Waqued ^{b,1}, Hem R. Thapa ^c, Arum Han ^{b,d}, Vladislav V. Yakovlev ^{b,e}, Jaan Laane ^a, Timothy P. Devarenne ^{c,*}

^a Department of Chemistry, Texas A&M University, College Station, TX, United States

^b Department of Biomedical Engineering, Texas A&M University, College Station, TX, United States

^c Department of Biochemistry & Biophysics, Texas A&M University, College Station, TX, United States

^d Department of Electrical & Computer Engineering, Texas A&M University, College Station, TX, United States

^e Department of Physics & Astronomy, Texas A&M University, College Station, TX, United States

ARTICLE INFO

Article history:

Received 30 August 2016

Received in revised form

27 September 2016

Accepted 28 September 2016

Available online 28 September 2016

Keywords:

Botryococcus braunii

DFT calculations

Lycopadiene

Raman spectroscopy

Tetraterpenoids

ABSTRACT

The green microalga *Botryococcus braunii* produces large amounts of liquid hydrocarbons that can be used as a renewable source for producing transportation fuels. In the L race of *B. braunii* the tetraterpene known as lycopadiene accumulates as the main hydrocarbon. Lycopadiene biosynthesis begins with the production of the eight carbon-carbon double bond (C=C) containing molecule lycopaoctaene, which is reduced to lycopadiene through four intermediates containing less C=C bonds. While the biosynthetic pathway for these hydrocarbons has recently been deciphered, a spectroscopic understanding of the molecular structure for these molecules remains to be reported. Here we describe the vibrational frequency assignments for all six L race hydrocarbons using density functional theory (DFT) calculations, showing that these molecules have between 312 and 348 vibrational frequencies. Experimental Raman spectroscopy analysis shows the regions for $\nu(\text{C}=\text{C})$ stretch and CH_2/CH_3 bending vibrations offer unique spectral signatures allowing for the differentiation of several of the hydrocarbons from each other.

© 2016 Elsevier B.V. All rights reserved.

1. Introduction

The colonial green microalga *Botryococcus braunii* is well known for producing large amounts of liquid hydrocarbon oils that can be readily converted into petroleum-equivalent combustion engine fuels [1–3]. These hydrocarbons are produced inside the *B. braunii* cells and secreted out of the cells into an extracellular matrix (ECM) that holds the cells into a colony [4]. The ECM acts as a reservoir for the hydrocarbons and contains 95% of all hydrocarbons found in the colony, allowing the *B. braunii* colonies to float within the water column [2,5–8]. Interestingly, *B. braunii* hydrocarbons have been shown through geologic time to be a major contributor to the formation of currently used fossil-fuel deposits [9–13].

B. braunii is divided into three separate chemical races, A, B, and L, that are defined by the type of hydrocarbon oils produced [1]. The focus of this study, the L race, produces the isoprenoid pathway-

derived C_{40} tetraterpenoid known as lycopadiene as the major accumulating hydrocarbon (Fig. 1) [14,15]. We recently deciphered the biosynthetic pathway for lycopadiene [16], which begins with the condensation of two molecules of the C_{20} isoprenoid intermediate geranylgeranyl diphosphate (GGPP) to produce the eight carbon-carbon double-bond (C=C)-containing lycopaoctaene (Fig. 1). This reaction is carried out by the enzyme lycopaoctaene synthase (LOS; Fig. 1). Successive reduction of lycopaoctaene by an unknown enzyme(s) through several lower number C=C bond containing intermediates of lycopahexaene, lycopapentaene, lycopatetraene, and lycopatriene finally produces the main lycopadiene hydrocarbon (Fig. 1). Lycopadiene constitutes 95% of all L race hydrocarbons with the intermediates accounting for the remaining 5% [16].

The different positions of the C=C bonds in the L race hydrocarbons should offer unique spectral qualities for these molecules to allow differentiation of each molecule by spectral approaches such as Raman spectroscopy. For example, lycopaoctaene contains C=C bonds at carbons 2, 6, 10, 14, 18, 22, 26, and 30 (Fig. 1), and reduction of lycopaoctaene to lycopadiene through the intermediates with less C=C bonds requires reduction on one side of

* Corresponding author.

E-mail address: tpd8@tamu.edu (T.P. Devarenne).

¹ These authors contributed equally to this study.

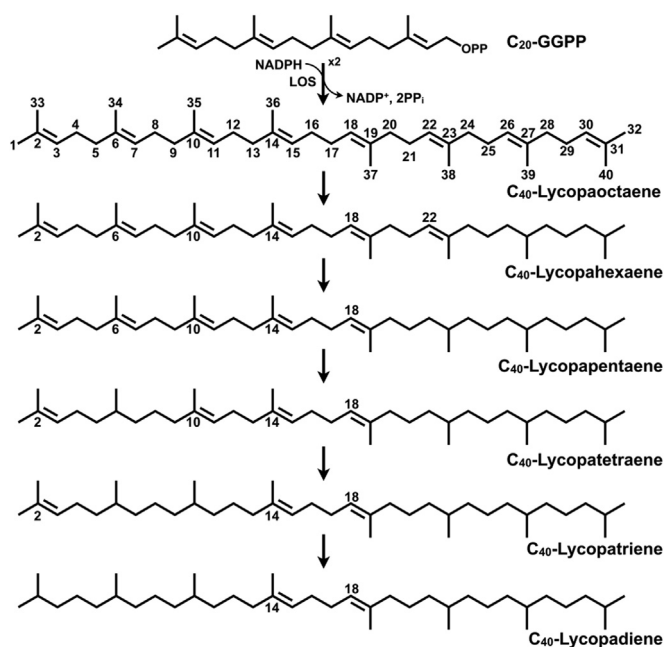


Fig. 1. The biosynthetic pathway for lycopadiene in the L race of *B. braunii*. Carbon position numbers given for lycopaoctaene apply to all other molecules where only the carbon position numbers are given for C=C bonds.

the molecule first, at carbons 22, 26, and 30, followed by reduction at carbons 2, 6, and 10 (Fig. 1). Using the B race of *B. braunii* that produces the triterpene hydrocarbons known as botryococcenes we have shown that Raman spectroscopy and density functional theory (DFT) calculations can distinguish between different C=C bonds within the botryococcene structure [17]. Thus, the different C=C bonds in the L race hydrocarbons should allow for distinguishing each molecule by Raman spectroscopy, which will be useful in future studies using noninvasive approaches such as confocal Raman microscopy to map the location of each hydrocarbon *in vivo*. Here we report the use of DFT calculations to assign frequencies to the bonds in each of the L race hydrocarbons and show that Raman spectroscopy can discriminate between several of these hydrocarbons.

2. Experimental methods

2.1. Culturing of *B. braunii*

B. braunii race L, Songkla Nakarin strain [14], was grown in modified Chu 13 media [18] at 22 °C under continuous aeration with filter-sterilized air enriched with 2.5% CO₂. Cultures were exposed to a 12:12 h light:dark cycle with a light intensity of 120 μmole photons·m⁻²·s⁻¹. Algal cultures were subcultured using 100 ml of floating colonies from a 6-week-old culture for inoculation into 750 ml of fresh medium.

2.2. Hydrocarbon purification

B. braunii L race hydrocarbons were purified as previously described [16]. Briefly, algal colonies were harvested using vacuum filtration through a 10 μm nylon mesh, freeze-dried, treated twice with *n*-hexane to extract extracellular hydrocarbons, followed by two treatments with CHCl₃:MeOH (2:1) to extract intracellular hydrocarbons. Solvents from both extracts were removed using a rotary evaporator, the hydrocarbons resuspended in *n*-hexane, and

each extract applied to separate gravity-fed silica gel columns using *n*-hexane as the mobile phase. The eluent from each column prior to the pigment front was collected and pooled as the total hydrocarbon fraction. The solvent was removed using a rotary evaporator, the hydrocarbons resuspended in a small amount of *n*-hexane, and individual hydrocarbons purified by HPLC using a Develosil 60 silica column (20 mm × 250 mm) with *n*-hexane as the mobile phase at a flow rate of 6 ml/min and detection at 210 nm. Purity to at least 95% and molecular mass of each isolated hydrocarbon was determined by GC-MS, and molecular structure determined by NMR as previously described [16].

2.3. Raman spectroscopy

Aliquots of purified hydrocarbons dissolved in *n*-hexane were spotted on a quartz glass slide and the solvent allowed to evaporate for 20 min prior to analysis. The Raman spectrum of each molecule was collected using a Horiba LabRAM HR Evolution Raman system with a 532 nm laser at 100% power with an output power of 107.9 mW. The laser was focused using a 100× objective lens with a 200 μm confocal hole and was dispersed by grating at 1800 lines per mm to collect the Raman spectra. The spectrum for each molecule was collected for 20 s with four accumulations in each collection window.

2.4. Theoretical computations

The vibrational frequencies of the six *B. braunii* L race hydrocarbons along with their Raman intensities were calculated using the Gaussian 09 program, Revision A.02 [19]. The DFT B3LYP method [20,21] was applied with a cc-pVTZ basis set for the computations. The calculations were done for the vapor-phase, but little difference between these values and those for the liquid state is expected. The Raman intensities were computed using the standard Gaussian 09 protocol and the bandwidths used for the computed spectra in the figures used the Gaussian default values. The Semichem AMPAC/AGUI program [22] was used to visualize the vibrational modes. A scaling factor of 0.968 was used for the vibrations of interest. In our previous work this scaling factor value was found to be best suited for correlating the experimental and theoretical frequency values [17,23]. Our previous work also showed that the different types of C=C stretching frequencies changed insignificantly for different conformational orientations of these types of molecules.

3. Results and discussion

3.1. Density function theory (DFT) computations for Raman spectra of L race hydrocarbons

These molecules are very large and possess a large number of vibrations resulting in very complex spectra. The individual vibrational assignments are too lengthy to detail, but Table 1 presents a summary of the types of vibrations for each molecule. The computed spectra themselves are presented in Fig. 2A. The focus of this study is the application of Raman spectroscopy to the identification of these molecules and to distinguish between them. The most useful spectral region for this study is the ν(C=C) stretch region in the 1600 to 1700 cm⁻¹ range. Fig. 2B shows the wavenumber positions and calculated intensities of the Raman bands for these molecules within a focused region of this ν(C=C) stretch region, between 1660 and 1680 cm⁻¹. Each of these molecules has a strong band between 1665 and 1668 cm⁻¹, but the difference between each of these bands is small (Fig. 2B). In addition, as can be seen, there are a number of weaker lines which differ in frequency

Table 1
Vibrations of *B. braunii* L race hydrocarbons.

Symbol	Vibration	Lycopaoctaene (C ₄₀ H ₆₆)		Lycopahexaene (C ₄₀ H ₇₀)		Lycopapentaene (C ₄₀ H ₇₂)		Lycopatetraene (C ₄₀ H ₇₄)		Lycopatriene (C ₄₀ H ₇₆)		Lycopadiene (C ₄₀ H ₇₈)	
		Wavenumber range (cm ⁻¹)	Number of vibrations	Wavenumber range (cm ⁻¹)	Number of vibrations	Wavenumber range (cm ⁻¹)	Number of vibrations	Wavenumber range (cm ⁻¹)	Number of vibrations	Wavenumber range (cm ⁻¹)	Number of vibrations	Wavenumber range (cm ⁻¹)	Number of vibrations
ν (CH ₃)	CH ₃ stretch	2899–3022	30	2880–3022	30	2880–3022	30	2881–3022	30	2878–3022	30	2879–3021	30
δ (CH ₃)	CH ₃ deformation	1271–1459	30	1289–1466	30	1291–1467	30	1274–1467	30	1274–1467	30	1274–1467	30
ρ (CH ₃)	CH ₃ rock	843–1252	20	840–1284	20	931–1279	20	828–1270	20	793–1270	20	801–1269	20
τ (CH ₃)	CH ₃ torsion	69–208	10	72–253	10	71–254	10	78–246	10	83–247	10	85–251	10
ν (CH ₂)	CH ₂ stretch	2899–3022	28	2880–3022	32	2880–3022	34	2881–3022	36	2878–3022	38	2879–3021	40
δ (CH ₂)	CH ₂ deformation	1427–1459	14	1427–1466	16	1426–1467	17	1427–1467	18	1427–1467	19	1430–1467	20
ω (CH ₂)	CH ₂ wag	1238–1319	14	1219–1371	16	1092–1380	17	1063–1377	18	1062–1378	19	1061–1379	20
t (CH ₂)	CH ₂ twist	1118–1276	14	1014–1353	16	1019–1330	17	987–1329	18	1001–1329	19	945–1339	20
ρ (CH ₂)	CH ₂ rock	727–957	14	716–1006	16	715–964	17	715–943	18	714–964	19	714–963	20
ν (CH)	=C-H stretch	2900–3022	8	2899–3022	6	2898–3022	5	2898–3022	4	2897–3022	3	2896–3021	2
ν (CH)	-C-H stretch	–	0	2880–2993	2	2880–2994	3	2881–2992	4	2878–2992	5	2879–2994	6
ω _i (CH)	CH wag (in-plane)	1028–1459	8	808–1459	8	803–1458	8	1021–1456	8	1001–1457	8	958–1456	8
ω _o (CH)	CH wag (out-of-plane)	740–1030	8	734–1030	8	727–1372	8	727–1358	8	736–1342	8	756–1345	8
ν (C=C)	C=C stretch	1665–1677	8	1666–1677	6	1666–1678	5	1667–1679	4	1668–1678	3	1668–1671	2
ν (C-C)	C-C stretch	727–1378	31	716–1379	33	715–1380	34	715–1377	35	714–1378	36	714–1379	37
b (C-C-C)	C-C-C angle bend	117–588	14	157–586	17	144–586	19	129–586	21	131–582	23	130–584	24
b (C=C-C)	C-C-C angle bend	272–588	14	270–586	11	268–586	9	266–586	7	262–582	5	260–584	4
ω _o (C-CH ₃)	C-CH ₃ wag (out-of-plane)	434–508	10	429–511	10	409–510	10	419–508	10	407–488	10	406–474	10
ω _i (C-CH ₃)	C-CH ₃ wag (in-plane)	348–427	10	351–424	10	348–429	10	332–407	10	302–393	10	301–390	10
τ (C-C)	Internal rotation (C-C)/ Skeletal	4–208	21	3–253	22	4–254	23	4–246	24	4–247	25	4–251	25
τ (C=C)	Internal rotation (C=C)/ Skeletal	48–208	6	50–253	5	49–254	4	42–246	3	43–247	2	45–251	2
Total		312		324		330		336		342		348	

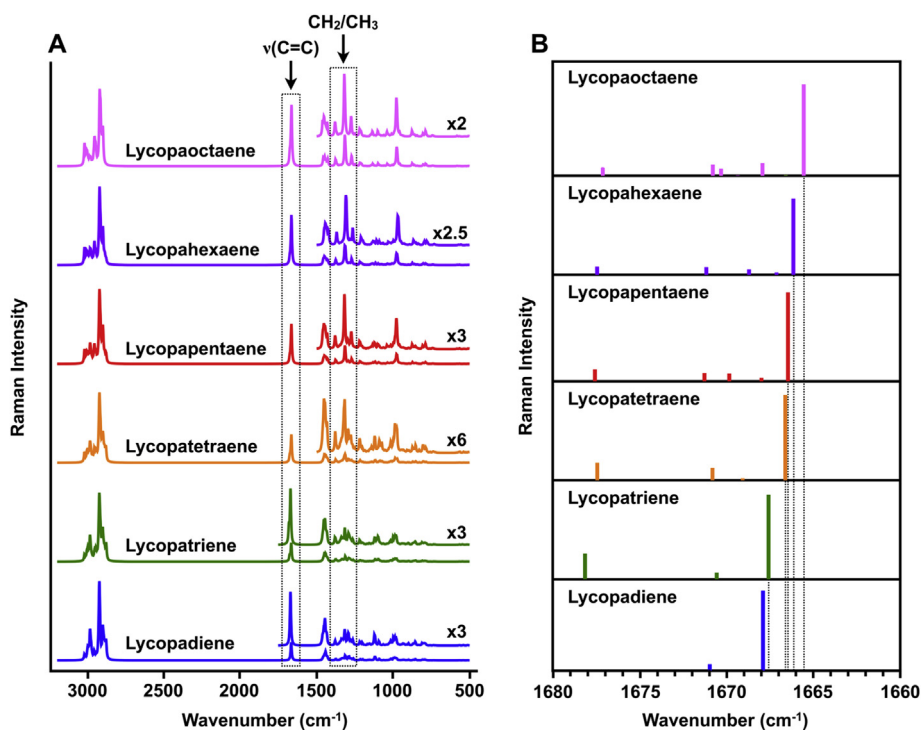


Fig. 2. Calculated spectra for *B. braunii* L race hydrocarbons. **A.** The calculated full Raman spectra for each hydrocarbon. Regions in dashed line boxes indicate the $\nu(\text{C}=\text{C})$ stretch region highlighted in **B** and further analyzed in Fig. 4, and CH_2/CH_3 bending analyzed in Fig. 4. **B.** The computation line spectra for the $\nu(\text{C}=\text{C})$ stretch region between 1660 and 1680 cm^{-1} .

and intensity from molecule to molecule (Fig. 2B). These computed Raman line positions are helpful in analyzing the experimental spectra.

3.2. Experimental Raman spectra of L race hydrocarbons and comparison to calculated spectra

The identified frequencies from the DFT calculations (Table 1) indicate that several spectral regions should offer molecule-specific signatures that could be used to distinguish the L race hydrocarbons from each other. Based on Table 1, the calculated spectra in Fig. 2, and our past Raman spectroscopy studies on the *B. braunii* B race hydrocarbons [17] and the triterpene molecule squalene [23], the spectral regions corresponding to $\nu(\text{C}=\text{C})$ stretch between 1600 and 1700 cm^{-1} and the region between 1250 and 1400 cm^{-1} which mainly contains CH_2/CH_3 bending vibrations, but also $\omega_1(\text{CH})$ wag (in-plane) and $\nu(\text{C}-\text{C})$ stretch, should offer some vibrational differences between each molecule. Additionally, these regions should offer a level of molecule specificity since the only difference between the molecular structure of each L race hydrocarbon is the position and number of $\text{C}=\text{C}$ bonds (Fig. 1). To test this experimentally, each L race hydrocarbon was analyzed individually by Raman spectroscopy and the spectra show high similarity across the spectra for each molecule (Fig. 3). In the $\nu(\text{C}=\text{C})$ stretch region lycopadiene, lycopatetraene, and lycopapentaene contain a single Raman band, while the spectra for lycopatriene, lycopahexaene, and lycopaoctaene contain a Raman band doublet (Fig. 3). The CH_2/CH_3 bending region for each molecule appears very similar except for lycopapentaene, which contains several bands not seen in the other spectra (Fig. 3).

A detailed analysis of these two regions of the experimental Raman spectra and a comparison with the calculated spectra indicates these regions can be used to distinguish several of the L race hydrocarbons from the others (Fig. 4). For the $\nu(\text{C}=\text{C})$ stretch region

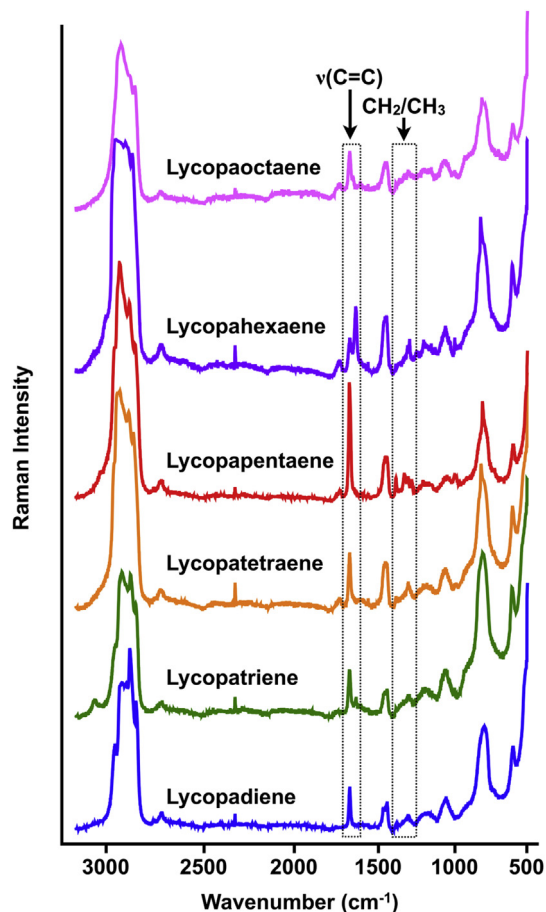


Fig. 3. Experimental Raman spectra for *B. braunii* L race hydrocarbons. Spectral regions for $\nu(\text{C}=\text{C})$ stretch and CH_2/CH_3 bending analyzed in Fig. 4 are shown in dashed line boxes.

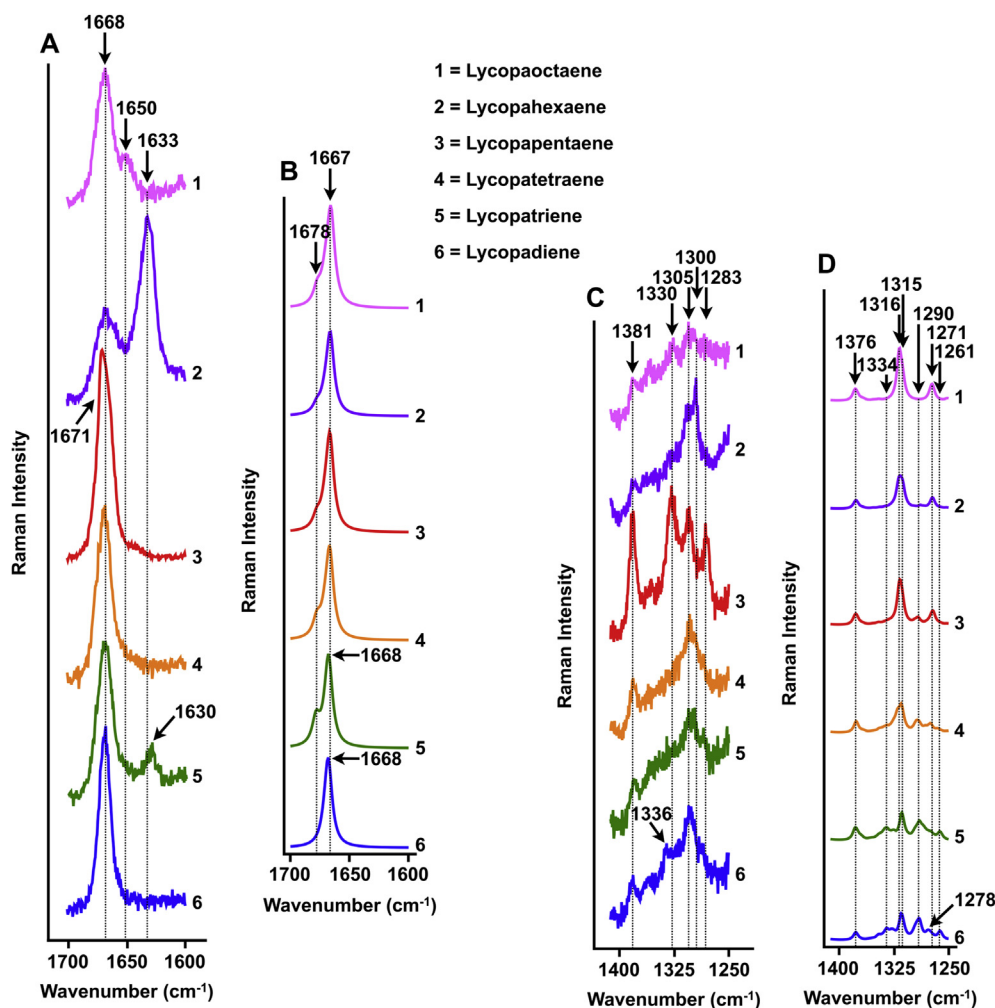


Fig. 4. Specific regions of the calculated and experimental Raman spectra for the *B. braunii* L race hydrocarbons. **A.** Experimental spectral region for $\nu(\text{C}=\text{C})$ stretch. **B.** Calculated spectral region for $\nu(\text{C}=\text{C})$ stretch. **C.** Experimental spectra region containing $\delta(\text{CH}_3)$ deformation, $\rho(\text{CH}_3)$ rock, $\omega(\text{CH}_2)$ wag, $t(\text{CH}_2)$ twist, $\omega_1(\text{CH})$ wag (in-plane), and $\nu(\text{C}-\text{C})$ stretch. **D.** Calculated spectra region containing $\delta(\text{CH}_3)$ deformation, $\rho(\text{CH}_3)$ rock, $\omega(\text{CH}_2)$ wag, $t(\text{CH}_2)$ twist, $\omega_1(\text{CH})$ wag (in-plane), and $\nu(\text{C}-\text{C})$ stretch.

(1600–1700 cm^{-1}) there is a strong band seen at 1668 cm^{-1} that is found in all hydrocarbons (Fig. 4A). This band is slightly shifted to 1671 cm^{-1} for lycopapentaene (Fig. 4A) and may be useful as a diagnostic signal for distinguishing this molecule from the other hydrocarbons. For lycophaxaene the predominant $\nu(\text{C}=\text{C})$ stretch Raman band is seen at 1633 cm^{-1} , which is not seen in any other hydrocarbon (Fig. 4A) and could be used to differentiate lycophaxaene from the other hydrocarbons. For lycopatriene this band is slightly shifted to 1630 cm^{-1} (Fig. 4A). It should be noted that these two bands in lycophaxaene and lycopatriene are not predicted by the DFT calculations (Fig. 4B), thus they may be due to laser decomposition products formed during analysis. Finally, a band at 1650 cm^{-1} in lycopaoctaene is not seen in any other hydrocarbon (Fig. 4A) and could be considered a diagnostic signal for this molecule.

It should be noted the DFT calculations predict that each hydrocarbon should have a number of $\nu(\text{C}=\text{C})$ stretch vibrations equal to the number of $\text{C}=\text{C}$ bonds in the molecule, and thus the same number of experimental Raman bands; i.e. 8 $\nu(\text{C}=\text{C})$ stretch vibrations for lycopaoctaene (Table 1). Additionally, the DFT calculations predict a Raman band at 1678 cm^{-1} for several of the hydrocarbons (Fig. 4B). In the experimental Raman spectroscopy (Fig. 4B) all predicted $\nu(\text{C}=\text{C})$ stretch bands are not seen likely due to spectral overlap between these bands caused by $\text{C}=\text{C}$ vibrations

within very close frequencies, which experimentally produces one or two predominant bands as shown in Fig. 4A. This is confirmed by the calculated spectra (Fig. 4B) and from our previous studies of $\nu(\text{C}=\text{C})$ stretch vibrations for the *B. braunii* B race botryococcene hydrocarbons [17] and for squalene [23].

For the CH_2/CH_3 bending region (1250–1400 cm^{-1}) most hydrocarbons show very similar experimental Raman spectra with predominant bands at 1381 cm^{-1} and 1305 cm^{-1} (Fig. 4C). However, lycopapentaene can be clearly distinguished from the other molecules based on the presence of CH_2/CH_3 bending Raman bands at 1330 cm^{-1} and 1283 cm^{-1} specific to this molecule (Fig. 4C). Both lycopapentaene and lycophaxaene could be differentiated from the other molecules based on the 1300 cm^{-1} band found in both of these molecules (Fig. 4C). Again, the DFT calculations predict many CH_2/CH_3 bending vibrations in the 1250–1400 cm^{-1} region (Table 1) that likely cannot be distinguished experimentally due to spectral overlap. The calculated spectra show a similar trend for each molecule in that four predominant Raman bands are predicted for lycopapentaene at 1376, 1316, 1290, and 1271 cm^{-1} (Fig. 4D), which are close to those seen in the experimental spectra (Fig. 4C). Lycopatetraene, lycopatriene, and lycopadiene show a slight shift to 1315 cm^{-1} in the predicted main Raman band (Fig. 4D). Many of these predicted bands are not seen for all molecules in the experimental spectra likely due to spectral overlap and high background (Fig. 4C).

4. Conclusions

The hydrocarbons from the L race of *B. braunii* are important molecules with industrial applications for producing transportation fuels [1,2], but their structural features based on spectrometry are not well understood. To address this we have analyzed the L race hydrocarbons by DFT calculations and Raman spectroscopy. These studies show that several of the analyzed hydrocarbons can be experimentally distinguished from each other using Raman spectroscopy. This information could be valuable in approaches such as using confocal Raman microscopy to map hydrocarbon biosynthesis locations in live *B. braunii* colonies/cells, or developing Raman spectroscopy-based systems for monitoring hydrocarbon production to determine optimal hydrocarbon production levels to inform harvest times.

Acknowledgments

This work was supported by the National Science Foundation [grant number EFRI-PSBR #1240478 to AH and TPD] and the Robert A. Welch Foundation [grant A-0396 to JL]. Computations were carried out on the Texas A&M Department of Chemistry Medusa computer system funded by the National Science Foundation [grant CHE-0541587].

References

- [1] P. Metzger, C. Largeau, *Botryococcus braunii*: a rich source for hydrocarbons and related ether lipids, *Appl. Microbiol. Biotechnol.* 66 (2005) 486–496.
- [2] A. Banerjee, R. Sharma, Y. Chisti, U.C. Banerjee, *Botryococcus braunii*: a renewable source of hydrocarbons and other chemicals, *Crit. Rev. Biotechnol.* 22 (2002) 245–279.
- [3] L.W. Hillen, G. Pollard, L.V. Wake, N. White, Hydrocracking of the oils of *Botryococcus braunii* to transport fuels, *Biotechnol. Bioeng.* 24 (1982) 193–205.
- [4] T.L. Weiss, R. Roth, C. Goodson, S. Vitha, I. Black, P. Azadi, J. Rusch, A. Holzenburg, T.P. Devarenne, U. Goodenough, Colony organization in the green alga *Botryococcus braunii* (Race B) is specified by a complex extracellular matrix, *Eukaryot. Cell* 11 (2012) 1424–1440.
- [5] J.R. Maxwell, A.G. Douglas, G. Eglinton, A. McCormick, Botryococcones-hydrocarbons of novel structure from the alga *Botryococcus braunii* Kützing, *Phytochem* 7 (1968) 2157–2171.
- [6] B.A. Knights, A.C. Brown, E. Conway, B.S. Middleditch, Hydrocarbons from the green form of the freshwater alga *Botryococcus braunii*, *Phytochem* 9 (1970) 1317–1324.
- [7] P. Metzger, M. David, E. Casadevall, Biosynthesis of triterpenoid hydrocarbons in the B-race of the green alga *Botryococcus braunii*. Sites of production and nature of the methylating agent, *Phytochem* 26 (1987) 129–134.
- [8] F.R. Wolf, A.M. Nonomura, J.A. Bassham, Growth and branched hydrocarbon production in a strain of *Botryococcus braunii* (Chlorophyta), *J. Phycol.* 21 (1985) 388–396.
- [9] J.M. Moldowan, W.K. Seifert, First discovery of botryococcones in petroleum, *J.C.S. Chem. Commun.* 19 (1980) 912–914.
- [10] D.M. McKirdy, R.E. Cox, J.K. Volkman, V.J. Howell, Botryococcones in a new class of Australian non-marine crude oils, *Nature* 320 (1986) 57–59.
- [11] E. Lichtfouse, S. Derenne, A. Mariotti, C. Largeau, Possible algal origin of long-chain odd *n*-alkanes in immature sediments as revealed by distributions and carbon-isotope ratios, *Org. Geochem.* 22 (1994) 1023–1027.
- [12] M. Glikson, K. Lindsay, J. Saxby, *Botryococcus* - a planktonic green alga, the source of petroleum through the ages: transmission electron microscopical studies of oil shales and petroleum source rocks, *Org. Geochem.* 14 (1989) 595–608.
- [13] P. Adam, P. Schaeffer, P. Albrecht, C₄₀ monoaromatic lycopane derivatives as indicators of the contribution of the alga *Botryococcus braunii* race L to the organic matter of Messel oil shale (Eocene, Germany), *Org. Geochem.* 37 (2006) 584–596.
- [14] P. Metzger, E. Casadevall, Lycopadiene, a tetraterpenoid hydrocarbon from new strains of the green alga *Botryococcus braunii*, *Tetrahedron Lett.* 28 (1987) 3931–3934.
- [15] P. Metzger, B. Allard, E. Casadevall, C. Berkloff, A. Coute, Structure and chemistry of a new chemical race of *Botryococcus braunii* (Chlorophyceae) that produces lycopadiene a tetraterpenoid hydrocarbon, *J. Phycol.* 26 (1990) 258–266.
- [16] H.R. Thapa, M.T. Naik, S. Okada, K. Takada, I. Molnar, Y. Xu, T.P. Devarenne, A squalene synthase-like enzyme initiates production of tetraterpenoid hydrocarbons in *Botryococcus braunii* Race L, *Nat. Commun.* 7 (2016) 11198.
- [17] T.L. Weiss, H.J. Chun, S. Okada, S. Vitha, A. Holzenburg, J. Laane, T.P. Devarenne, Raman spectroscopy analysis of botryococcones hydrocarbons from the green microalga *Botryococcus braunii*, *J. Biol. Chem.* 285 (2010) 32458–32466.
- [18] S.P. Chu, The influence of the mineral composition of the medium on the growth of planktonic algae Part 1. Methods and culture media, *J. Ecol.* 30 (1942) 284–325.
- [19] M.J. Frisch, G.W. Trucks, H.B. Schlegel, G.E. Scuseria, M.A. Robb, J.R. Cheeseman, G. Scalmani, V. Barone, B. Mennucci, G.A. Petersson, H. Nakatsuji, M. Caricato, X. Li, H.P. Hratchian, A.F. Izmaylov, J. Bloino, G. Zheng, J.L. Sonnenberg, M. Hada, M. Ehara, K. Toyota, R. Fukuda, J. Hasegawa, M. Ishida, T. Nakajima, Y. Honda, O. Kitao, H. Nakai, T. Vreven, J.A. Montgomery Jr., J.E. Peralta, F. Ogliaro, M. Bearpark, J.J. Heyd, E. Brothers, K.N. Kudin, V.N. Staroverov, R. Kobayashi, J. Normand, K. Raghavachari, A. Rendell, J.C. Burant, S.S. Iyengar, J. Tomasi, M. Cossi, N. Rega, J.M. Millam, M. Klene, J.E. Knox, J.B. Cross, V. Bakken, C. Adamo, J. Jaramillo, R. Gomperts, R.E. Stratmann, O. Yazyev, A.J. Austin, R. Cammi, C. Pomelli, J.W. Ochterski, R.L. Martin, K. Morokuma, V.G. Zakrzewski, G.A. Voth, P. Salvador, J.J. Dannenberg, S. Dapprich, A.D. Daniels, Ö. Farkas, J.B. Foresman, J.V. Ortiz, J. Cioslowski, D.J. Fox, Gaussian 09, Revision A.02, Gaussian, Inc., Wallingford CT, 2009.
- [20] A.D. Becke, Density-functional thermochemistry 3. The role of exact exchange, *J. Chem. Phys.* 98 (1993) 5648–5652.
- [21] C.T. Lee, W.T. Yang, R.G. Parr, Development of the Colle-Salvetti correlation-energy formula into a functional of the electron-density, *Phys. Rev. B* 37 (1988) 785–789.
- [22] I.S. AGUI Program from Semichem, 2016. KS 66216, <http://www.semichem.com/>.
- [23] H.J. Chun, T.L. Weiss, T.P. Devarenne, J. Laane, Vibrational spectra and DFT calculations of squalene, *J. Mol. Struct.* 1032 (2013) 203–206.